JEATSA JOURNAL
JOURNAL OF ENGINEERING ADVANCES AND TECHNOLOGIES FOR SUSTAINABLE APPLICATIONS
Volume 1, Issue 2 (April, 2025)
Print ISSN: 3062-5629 Online ISSN: 3062-5637
Open Access
https://jeats.journals.ekb.eg/

Mathematical Study On A Direct Contact Humidifier Of A Humidification-Dehumidification Desalination System

Mohamed Ashraf Galal, Raouf N. Abdelmessih, Ehab M. Mina
Department of Mechanical Power Engineering, Faculty of Engineering, Ain-Shams University, Cairo, Egypt

Mohamed_ashraf@eng.asu.edu.eg

Received 29-09-2024
Revised 16-10-2024
Accepted: 1-11-2024
Published: April-2025

Print ISSN: 3062-5629
Online ISSN: 3062-5637

Abstract- In a humidification-dehumidification (HDH) water desalination system, the humidifier is a significant component that directly impacts the overall process of producing fresh water from saline or brackish sources. In this study, a heat-mass transfer numerical model between the hot sprayed seawater and air on a direct contact humidifier was developed to investigate the effect of inlet seawater temperature, seawater mass flow rate, inlet air temperature, and air mass flow rate on humidifier effectiveness and freshwater evaporation rate. The results show that the optimum value of humidifier effectiveness is achieved on a unity mass flow rate ratio between seawater and air, and the seawater inlet temperature and the mass flow rate ratio between seawater and air are the most critical parameters influencing the productivity of the humidifier. The maximum value of water evaporation is 341 *kg/hr* that occurs at operating conditions of inlet seawater temperature of 90℃, inlet air temperature of 30℃, inlet air relative humidity of 50%, and seawater to air mass ratio of 5. The findings found that freshwater productivity improves by approximately 25% when the seawater temperature is increased by 10%.

Keywords- *heat and mass transfer, humidifier, humidification-dehumidification desalination, packing, direct contact.*

I. INTRODUCTION

Water is essential for all forms of life on Earth. It is a fundamental requirement for the survival, growth, and reproduction of plants, animals, and humans. From cellular processes to ecosystem functioning, water plays a vital role in maintaining life's biological processes. Water scarcity is a pressing global issue that leads to limited access to safe and clean drinking water for communities. This can result in compromised hygiene, increased risks of waterborne diseases, and negative impacts on public health. It allows for the utilization of abundant saline water resources, such as seawater or brackish water, effectively expanding the available water supply and reducing reliance on traditional freshwater sources. So, one of the methods for desalination is Humidification-Dehumidification (HDH) desalination, which can be employed to provide freshwater in small-scale community settings, particularly in remote or water-scarce areas where access to clean water is limited. These systems can serve as decentralized water treatment units, delivering freshwater for drinking and for agricultural productivity in arid or semi-arid regions. Also, HDH desalination is suitable for off-grid and remote applications, such as islands, coastal communities, or isolated facilities. Many studies have investigated different techniques for HDH systems. Here are some of the articles that presented research on this type.

Dehghani et al. [1] presented a theoretical investigation of the vapor compression heat pump coupled with the HDH desalination system of direct contact dehumidification. Several system performance indices including recovery ratio, coefficient of performance and specific electrical energy consumption were investigated under the influence of freshwater temperature, saline water temperature, mass flowrate ratio of saline water to air, and mass flowrate ratio of saline water to freshwater. Xu et al. [2] explored the performance of a solar-assisted heat pump desalination unit and found that the air outlet temperature plays a significant role in improving the humidification process. As the air temperature increases, the relative humidity decreases, allowing more water to evaporate and increasing the system's overall productivity. Ge et al. [3] conducted an experimental study that demonstrated how controlling the air outlet temperature can optimize the humidification process, particularly by ensuring that the temperature remains at a level that maximizes water vapor up-take without leading to excessive energy consumption. Rahimi-Ahar et al. [4] provided a comprehensive review of the air humidification-dehumidification process for desalination, emphasizing that the effectiveness of the humidifier is influenced by factors such as air-water contact time, surface area, and the temperature gradient between the water and air. Lawal et al. [5] discussed various strategies to enhance the effectiveness of humidifiers, such as optimizing the design of the packing material inside the humidifier, which increases the surface area for air-water contact and improves the fresh water productivity. Kabeel et al.

hackettes. Increasing seawater temperature significantly enhances humidification performance, with optimal performance achieved at temperatures above 80 °C. The study provides theoretical guidance for selecting efficient packing materials.

NOMENCLATURE

a_p	Specific surface area of the packing $\left(\frac{m^2}{m^3}\right)$
A_c	Cross-section area of the packing (m^2)
c_p	Specific heat $(\frac{\mathrm{J}}{\mathrm{kg.K}})$
α	Heat transfer coefficient $(\frac{\mathrm{W}}{m^2.\mathrm{K}})$
$\dot{m}_{ev}$	Total freshwater evaporation rate $(\frac{kg}{hr})$
$\dot{m}$	Mass flow rate $(\frac{kg}{s})$
dz	Step of the studied element height (m)
h_{fg}	Latent heat of vaporization $(\frac{\mathrm{J}}{kg})$
β	Mass transfer coefficient $(\frac{m}{\mathrm{s}})$
MR	Seawater to air mass flow rate ratio
T	Temperature (℃)
H	Enthalpy $(\frac{\mathrm{J}}{s})$

Greek Letters

ω	Humidity ratio $(\frac{kg_{wv}}{kg_{da}})$
ρ	Density $(\frac{kg}{m^3})$
ϕ	Relative humidity (%)
ε	Humidifier effectiveness

Subscripts

atm	Atmosphere
a	Dry air
int	Interface
p	Packing
sw	Seawater
ev	Evaporation
in	Inlet
o	Outlet

In the present work, we utilize a differential equation mathematical model to explore the control volume of the researched element of the direct contact humidifier through structured packing, hence optimizing the humidifier's performance by studying the effect of inlet seawater temperature, seawater mass flow rate, inlet air temperature and air mass flow rate on humidifier effectiveness and freshwater evaporation rate. After that, determine the optimum operating conditions to attain the highest output values.

II. SYSTEM DESCRIPTION

Fig. 1. shows the overview of the humidifier of a HDH desalination cycle. It contains a packing material, made of polypropylene, designed to provide a large surface area for air-water contact. This type of packing has the specific surface area of the packing material $a_p = 350 \left(\frac{m^2}{m^3}\right)$ and cross section area of the packing $A_c = 0.1\ (m^2)$ with height of 0.6 m. In HDH system, the hot saline water is sprayed over the packing bed through nozzles meeting the inlet air in counter direction. As the air passes over the wetted surfaces, it absorbs water vapor, increasing its humidity. As heat is supplied to the interface between air and water, it provides the latent heat needed to cause water molecules to leave the interface to the air stream, effectively separating the water from the dissolved salts

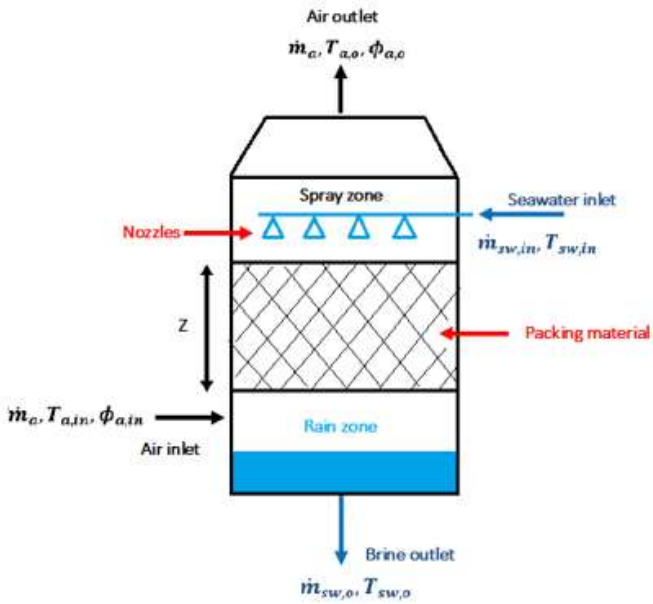

Figure 1: Schematic of the packed-bed direct-contact humidifier of a HDH desalination cycle.

Based on heat and mass transfer relations between air and sprayed seawater in a control volume of packing height which expressed in Fig.

2. The heat and mass transfer between an interface layer on the surface of the water and the bulk air controls the outputs of the computational element.

This model is solved based on a number of assumptions:

1. When the spray water and air inside the humidifier were thermally exchanging, the heat transfer between the humidifier and the surrounding air was ignored.
2. The seawater temperature must not be less than the inlet temperature of air.
3. Mass transfer and heat transfer areas were equivalent.
4. The heat and mass transfer process within the humidifier remains in a steady state.

The sensible heat extracted from the water element in terms of the energy balance on the water side is expressed in the form of:

$$\dot{Q}_{sensible,water} = \dot{m}_{sw}\, c_w\, dT_{sw} \quad (1)$$

The rate of heat transfer between the water and the interface is expressed in the form of:

$$\dot{Q}_{sensible,water} = h_w\, A_C\, a_p\, dz\ (T_{sw} - T_{int}) \quad (2)$$

where $\dot{m}_{sw}$is the mass flow rate of the water, c_w is the specific heat of the water, h_w is the convection coefficient in the side of the water, A_C is the cross-section are of the packing, a_p is specific surface area of the packing material, dz is the studied element height, dT_{sw} is the temperature difference of the inlet water to the studied element, and the temperature of the outlet water from the studied element, and T_{int} is the temperature of the interface

The sensible heat added to the air element in terms of the energy balance on the air side is expressed in the form of:

$$\dot{Q}_{sensible,air} = \dot{m}_a\, c_a\, dT_a \quad (3)$$

The rate of heat transfer between the air and the interface is expressed in the form of:

$$\dot{Q}_{sensible,air} = h_a\, A_C\, a_p\, dz\ (T_{int} - T_a) \quad (4)$$

where $\dot{m}_a$ is the mass flow rate of air, c_a is the specific heat of the air, h_a is the convection coefficient in the side of the air, dT_a is the temperature difference between of the inlet air to the studied element and temperature of the outlet air from the studied element which expected to increase on moving up the packing. The mass transfer of fresh water that transferred to the air is expressed in the form:

$$\dot{m}_{ev} = h_m\, A_C\, a_p\, dz\ (\omega_{int} - \omega_a) \quad (5)$$

The rate of freshwater evaporated in the air in terms of mass balance between inlet and outlet element is calculated from the equation:

$$\dot{m}_{ev} = \dot{m}_a\, d\omega_a \quad (6)$$

The latent heat that added to the air is expressed in the form:

$$\dot{Q}_{latent} = \dot{m}_{ev}\ h_{fg} \quad (7)$$

where m_{ev} is the mass flow rate of evaporated water in air, ω_{int} is the humidity ratio of interface, ω_a is the humidity ratio of air through the humidifier, h_{fg} is latent heat of vaporization and h_m is the mass transfer coefficient.

By applying energy balance between air and water:

$$\dot{Q}_{sensible,air} + \dot{Q}_{latent} = \dot{Q}_{sensible,water} \quad (8)$$

We get the values of dT_a(i), dT_{sw}(i), $d\omega_a$(i), and $d\dot{m}_{ev}$(i) by solving the previous equations simultaneously. These values are used to obtain the values of next step using Euler method.

For the upcoming steps, the following equations are used to express the change in each step by solving each element step using Newton Rapson method

$$T_a(\text{i+1}) = T_a(\text{i}) + dT_a(\text{i}) \quad (9)$$

$$T_{sw}(\text{i+1}) = T_{sw}(\text{i}) + dT_{sw}(\text{i}) \quad (10)$$

$$\omega_a(\text{i+1}) = \omega_a(\text{i}) + d\omega_a(\text{i}) \quad (11)$$

This model is valid to be applied to any assumption of inlet parameters for air and water inlet conditions. In reality, variations in these parameters can significantly influence the performance of the direct-contact humidifier, which will be discussed in the following results section. In addition, the model can be used successfully for a different humidifier geometry and different types of packing material properties.

The system performance is assessed using a variety of non-dimensional characteristics under different operating conditions. In the Humidifier, the mass flow rate ratio of seawater to air is crucial to the device's performance.

$$MR = \frac{\dot{m}_{sw}}{\dot{m}_a} \quad (12)$$

In the humidifier, The effectiveness of the component is defined as a comparison of the actual thermal energy against ideal thermal energy transferred from each stream and is expressed as the change of actual enthalpy rate to the maximum possible change in enthalpy rate [1]. Therefore, the humidifier's effectiveness would be denoted as follows:

$$\varepsilon = max\left(\frac{H_{a,o} - H_{a,in}}{\dot{H}_{a,o}^{ideal} - H_{a,in}}, \frac{H_{sw,in} - H_{sw,o}}{H_{sw,in} - \dot{H}_{sw,o}^{ideal}}\right) \quad (13)$$

In the humidifier, the ideal enthalpy of outlet air ($\dot{H}_{a,o}^{ideal}$) occurs when the exit air from the humidifier is totally saturated at the inlet seawater temperature and the ideal enthalpy of seawater ($\dot{H}_{sw,o}^{ideal}$) happens when its temperature is equal to the temperature of the inlet air.

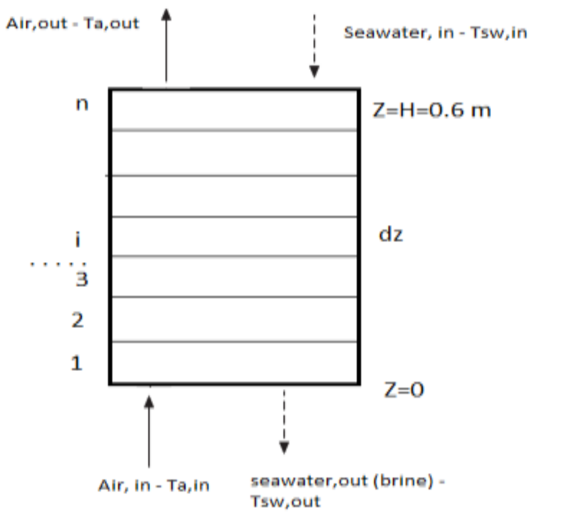

Figure 2: Schematic diagram of the humidifier control volume.

III. MODEL VALIDATION

The validation of the mathematical model proposed in this study is conducted by comparison with the study of the humidifier by Dehghani et al. [1] in Fig. 3. This humidifier has the same operating conditions, height of packing, and packing fill properties as the one being examined here. This validation is done for the working conditions of $T_{sw,in} = 70$ °C, $T_{a,in} = (22-44)$°C, $\phi_{a,in} = 100$ %, humidifier height of 2.25 m and packing specific area of $226\ m^2/m^3$. It was found that the maximum difference between the two models is about 2%. As shown in this figure, the humidifier effectiveness varies with the different values of mass flow rate ratio.

To check the accuracy and reliability of the model of this study, another validation was conducted with the experiments that were conducted by Zhang et al. [9] and numerical model that developed by Qundong Zhu et al. [8] was presented in Fig. 4. It is observed that under the same operation conditions ($\dot{m}_a = 1\ kg/s$, $T_{sw} = 50$°C, $T_a = 16$°C, $\phi_{a,in} = 10$ %), the average error is 3% from the experimental results, which is an acceptable error. The system's pertinent operational parameters were adjusted to examine the humidifier performance.

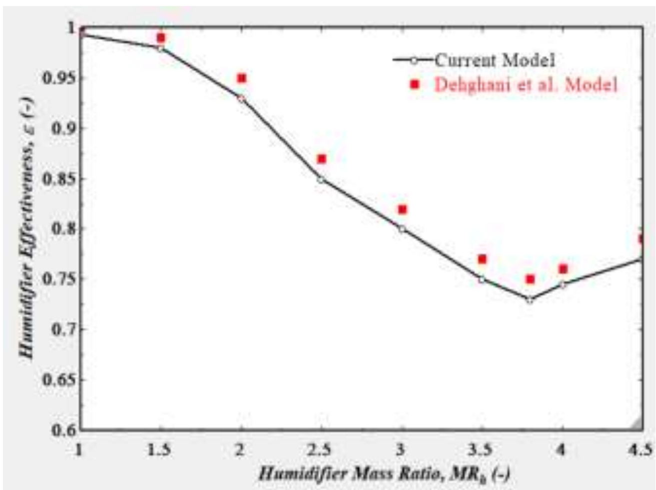

Figure 3: Comparison of the humidifier effectiveness between the numerical model in this paper and Dehghani et al. model [1]

JEATSA JOURNAL
JOURNAL OF ENGINEERING ADVANCES AND TECHNOLOGIES FOR SUSTAINABLE APPLICATIONS
Volume 1, Issue 2 (April, 2025)
Print ISSN: 3062-5629 Online ISSN: 3062-5637
Open Access
https://jeats.journals.ekb.eg/

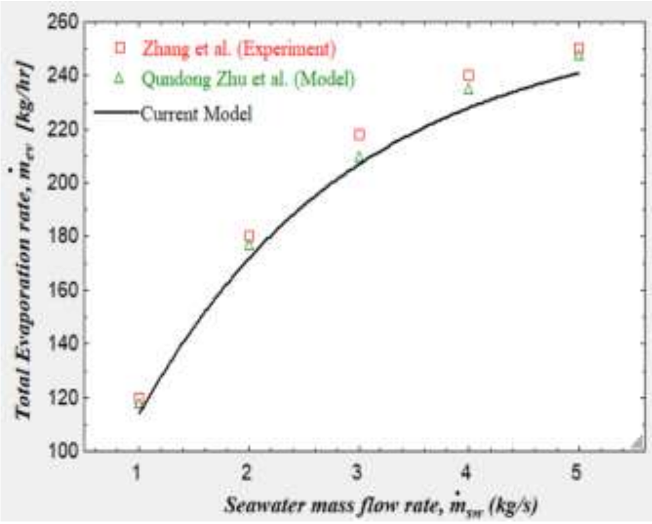

Figure 4: Comparison of the total freshwater evaporation rate between the numerical model in this paper, Zhang et al.[9] (experiment data) and Qundong Zhu et al. model [8]

IV. RESULT AND DISCUSSION

A. Effect of air mass flow rate on humidifier effectiveness and freshwater evaporation rate.

Fig. 5. shows the effect of air mass flow rate variation on humidifier effectiveness at different values of seawater mass flow rate, as shown that as the inlet air mass flow rate increases, the effectiveness can exhibit a decrease to a certain value, then, followed by an increase.

The ratio of seawater to air mass is large at lower values of air mass flow rates. This indicates that the air has enough time to absorb humidity from the seawater while it moves within the humidifier and that there is a significant volume of seawater with respect to the air. Due to the air's limited ability to capture both moisture and heat in comparison to the seawater that is readily accessible, air-side effectiveness is the limiting factor. Consequently, the effectiveness of the humidifier diminishes significantly when the air mass flow rate increases due to a decrease in the air-side heat and mass transfer rate.

The seawater-to-air mass ratio falls as the air mass flow rate rises, and the air in this area starts to be more efficient to absorb moisture and heat from the seawater. Nonetheless, all curves in this area exhibit a minimal effectiveness. This occurs because the heat and mass transfer between the water side and the air side are not precisely balanced. At higher seawater flow rates ($\dot{m}_{sw} = 2\ kg/s$), this lowest point is more noticeable because of the larger discrepancy in mass and heat transfer capabilities.

At higher values of air mass flow rates, the seawater-to-air mass ratio becomes low. Due to the seawater's restricted ability to supply heat and moisture in comparison to the air's ability to absorb it, seawater-side effectiveness now becomes the most restricting element. As the available seawater has been used more efficiently in this area, the humidifier's effectiveness rises with air mass flow rate. Because the air's absorption capacity increases dramatically while seawater stays constant, the rise is more pronounced at lower seawater flow rates ($\dot{m}_{sw} = 1\ kg/s$) As demonstrated, the optimal effectiveness is achieved when $\dot{m}_{sw} = 1 kg/s$, $\dot{m}_a = 1 kg/s$.

Fig. 6. illustrates the effect of the air mass flow rate variation on the total freshwater evaporation rate at different values of seawater mass flow rate which results that at a higher values of air flow rates, it can increase the overall evaporation rate because more air passes through the humidifier per unit time, even if each unit of air absorbs slightly less moisture. the graph shows that when seawater mass flow rate is doubled, the freshwater evaporation rate increases by 34% at $\dot{m}_a = 1\ kg/s$ and increases by 14% at $\dot{m}_a = 0.2\ kg/s$. This means that by increasing the water flow rates at lower air flow rates, the air side capability to absorb this energy is little affected, leading to minimal changes in freshwater productivity.

B. Effect of seawater mass flow rate on humidifier effectiveness and freshwater evaporation rate.

Fig. 7. displays the impact of the seawater mass flow rate variation on the humidifier effectiveness at different values of air mass flow rate. The effectiveness of a humidifier can exhibit a decrease followed by an increase as the seawater mass flow rate increases. The trend in this graph has the same behavior and explanation as Fig. 4.

Fig. 8. shows that the impact of the seawater mass flow rate variation on the total freshwater evaporation rate at different values of air mass flow rate which shows that a higher values of seawater flow rate can lead to an increased evaporation rate as more water is available to be evaporated

into the air.

C. Effect of inlet seawater temperature on humidifier effectiveness and freshwater evaporation rate.

Fig. 9. displays the effect of the inlet seawater temperature variation on the humidifier effectiveness at different values of seawater to air mass flow rate ratio. At low mass flow ratio (MR=1), the humidifier effectiveness remains almost constant across the entire range of inlet seawater temperatures. Increasing the seawater temperature enhances heat and mass transfer, but the air side's ability to absorb this energy is essentially unchanged. At higher mass flow rate ratios, the effectiveness decreases with increasing seawater temperatures and slightly increases at very high temperatures. In this case, the seawater flow rate is significantly higher than the air flow rate. As seawater temperature increases, the air becomes the limiting factor due to its limited capacity to absorb additional moisture. This difference leads to a decline in effectiveness. At very high temperatures, the seawater's vapor pressure is much higher and the increased thermal energy in the seawater boosts evaporation rates, improving humidification and improving the humidifier's effectiveness.

Fig. 10. illustrates the impact of change the inlet seawater temperature on the total freshwater evaporation rate at different values of seawater to air mass flow rate ratio. By increasing the inlet seawater temperature, the evaporation rate increases significantly because warmer water evaporates more readily.

D. Effect of inlet air temperature on humidifier effectiveness and freshwater evaporation rate.

Fig. 11. shows the effect of changing the inlet air temperature on humidifier effectiveness at different values of seawater to air mass flow rate ratio. Higher inlet air temperature generally enhances humidifier effectiveness because warmer air can hold more moisture, leading to more efficient evaporation. But, at very high mass flow rate ratio (MR=5), the effectiveness

Fig. 12. displays the impact of the inlet air temperature variation on the total freshwater evaporation rate at different values of seawater to air mass flow rate ratio. When the air temperature is increased, these gradients decrease if the water temperature remains constant. A smaller temperature difference reduces the heat transfer from the water to the air, which is the primary driver of evaporation. With less heat being transferred from the water to the air, the rate at which water molecules gain enough energy to evaporate is reduced.

A Sensitivity analysis was developed to determine the influence of key input parameters, including air mass flow rate, water mass flow rate, air inlet temperature, and water inlet temperature, on the freshwater evaporation rate. This analysis is critical for understanding parameter significance and optimizing the design of the HDH desalination system. The analysis was conducted by varying each input parameter individually by ±10% around its baseline value while keeping all other parameters constant.

The baseline values were based on the inlet operating conditions: $T_{sw,in}$ =60°C, $T_{a,in}$ =30°C, $\dot{m}_a = 0.5\ kg/s$, $\dot{m}_{sw} = 1\ kg/s, and\ \phi_{a,in} = 50\%$. Sensitivity index were calculated for each input parameter using:

$$Sensitivity\ Index\ (S) = \frac{Percentage\ change\ in\ output}{Percentage\ change\ in\ input}$$

The results found that the inlet seawater temperature had the highest influence on the freshwater evaporation rate ($S_{T_{sw}}$ = 2.47) while the air inlet temperature had the minimum impact on freshwater evaporation rate (S_{T_a}= -0.163). The air and seawater mass flow rate had a moderate influence on freshwater evaporation rate ($S_{\dot{m}_{a,in}}$=0.418, $S_{\dot{m}_{sw,in}}$= 0.355).

The high sensitivity of the freshwater evaporation rate to seawater temperature rate suggests that precise control of seawater temperature is essential for achieving optimal desalination performance.

JEATSA JOURNAL
JOURNAL OF ENGINEERING ADVANCES AND TECHNOLOGIES FOR SUSTAINABLE APPLICATIONS
Volume 1, Issue 2 (April, 2025)
Print ISSN: 3062-5629 Online ISSN: 3062-5637
Open Access
https://jeats.journals.ekb.eg/

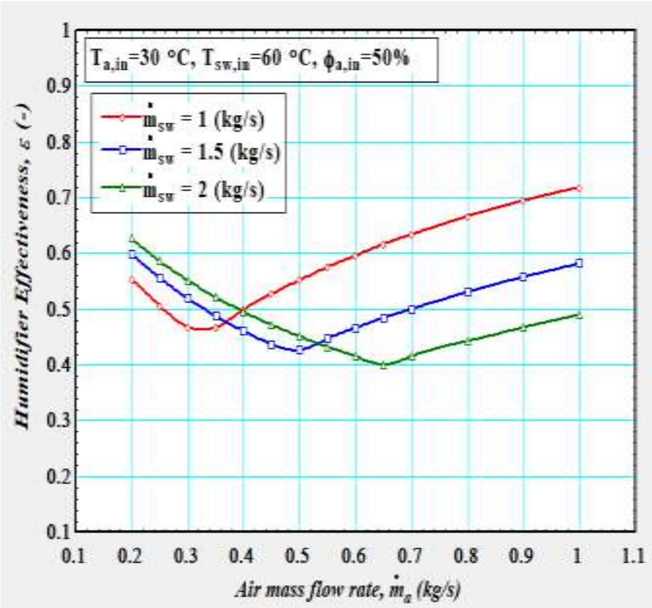

Figure 5: Variation of air mass flow rate on humidifier effectiveness at different values of seawater mass flow rate.

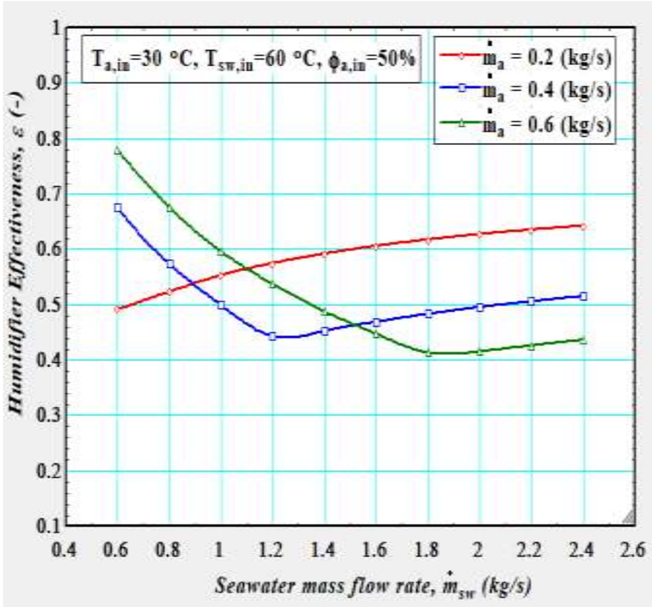

Figure 7: Variation of seawater mass flow rate on humidifier effectiveness at different values of air mass flow rate.

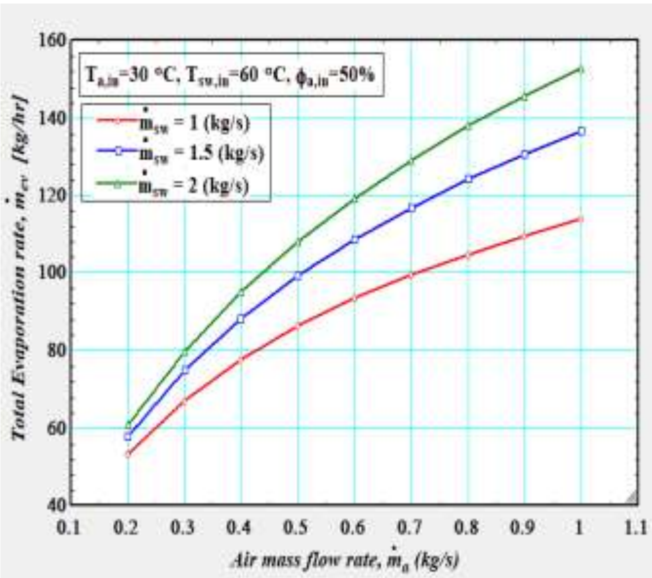

Figure 6: Variation of air mass flow rate on total freshwater evaporation rate at different values of seawater mass flow rate.

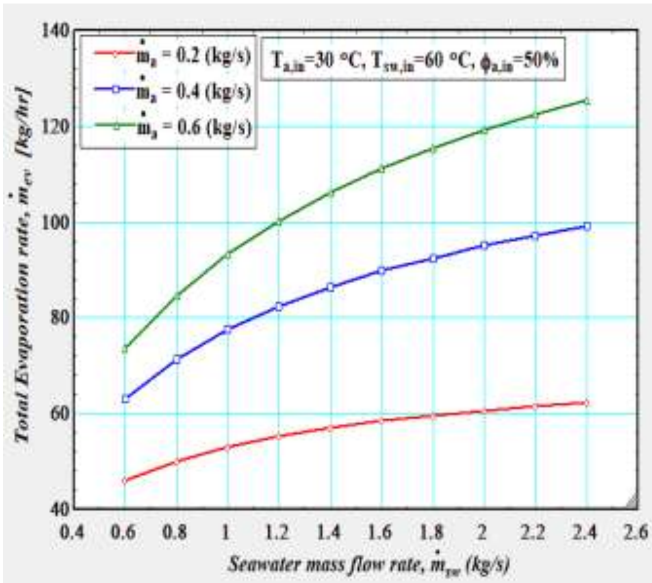

Figure 8: Variation of seawater mass flow rate on total freshwater evaporation rate at different values of air mass flow rate.

JEATSA JOURNAL
JOURNAL OF ENGINEERING ADVANCES AND TECHNOLOGIES FOR SUSTAINABLE APPLICATIONS
Volume 1, Issue 2 (April, 2025)
Print ISSN: 3062-5629 Online ISSN: 3062-5637
Open Access
https://jeats.journals.ekb.eg/

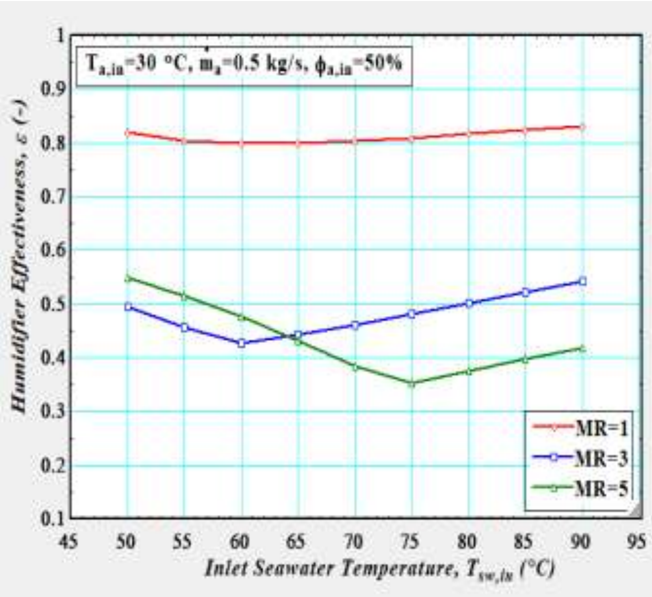

Figure 9: Variation of inlet seawater temperature on humidifier effectiveness at different values of seawater to air mass flow rate ratio.

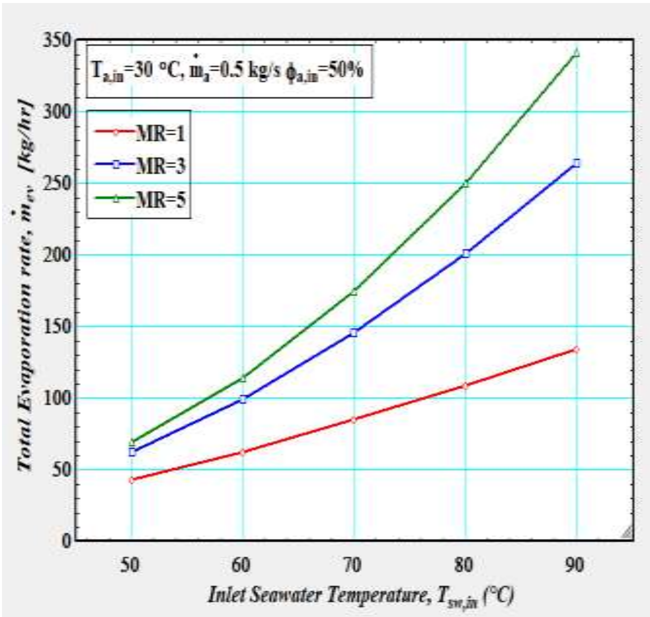

Figure 10: Variation of inlet seawater temperature on total freshwater evaporation rate at different values of seawater to air mass flow rate ratio.

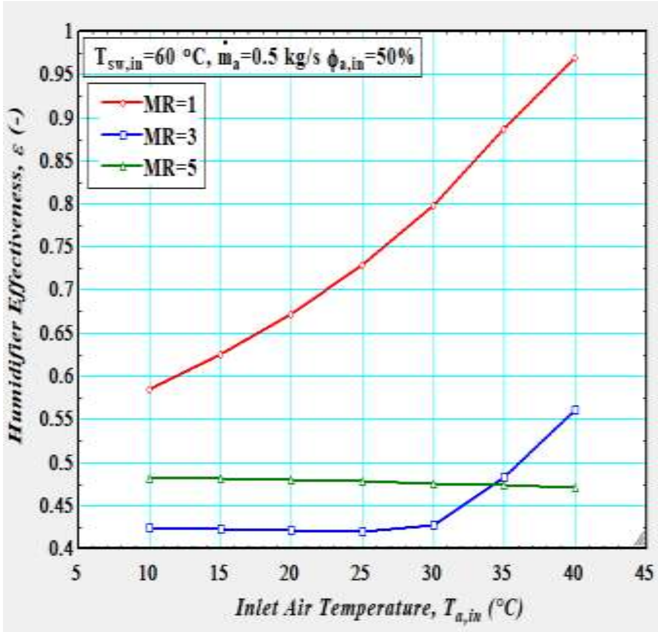

Figure 11: Variation of inlet air temperature on humidifier effectiveness at different values of seawater to air mass flow rate ratio.

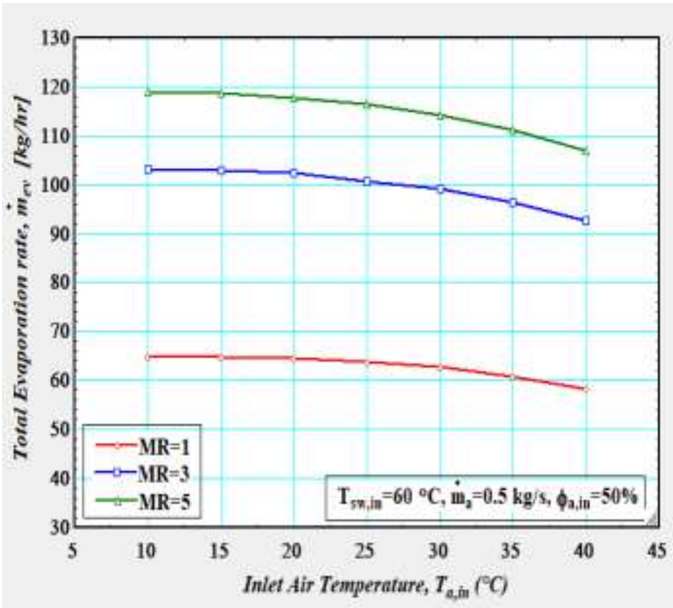

Figure 12: Variation of inlet air temperature on total freshwater evaporation rate at different values of seawater to air mass flow rate.

V. CONCLUSION

Mathematical modelling is used to examine the performance analysis of the direct contact humidifier. We may thus conclude that when the system operates in a way that results in a greater rate of water evaporation and humidifier effectiveness.

- Increases in the ratio of seawater to air mass flow rate result in maximum values of freshwater evaporation values.
- The optimum value of humidifier effectiveness is achieved on a unity mass flow rate ratio ($MR = 1$).
- Seawater inlet temperature and mass flow rate ratio are the most critical parameters influencing freshwater production rate.
- The low sensitivity of evaporation rate to air temperature suggests opportunities for energy savings by optimizing air heater operation.
- Freshwater productivity improves by approximately 25% when the seawater temperature is increased by 10%.
- The maximum value of water evaporation is 341 kg/hr. that occurs at operating conditions of $T_{sw,in}$=90°C, $T_{a,in}$=30°C, $MR = 5, and\ \phi_{a,in} = 50\%$.

This study presented a mathematical model for the direct-contact humidifier in a humidification-dehumidification (HDH) desalination system, providing valuable insights into its performance under various operating conditions. However, there are several opportunities for future research to enhance and expand upon this work:

- Future work could integrate the humidifier with other HDH desalination stages, like dehumidifiers, heat exchangers, and energy recovery units, for a holistic assessment of performance metrics such as gain output ratio and specific energy consumption.
- Future studies could include energy efficiency analysis, examining humidifier energy use under varying conditions and incorporating renewable sources like solar or waste heat to enhance sustainability.
- Optimizing humidifier performance could involve exploring advanced materials, like high-surface-area or improved wettability packing, and alternative designs to boost mass and heat transfer.
- Integrating the humidifier with hybrid desalination systems, such as HDH combined with reverse osmosis or multi-effect distillation, could create multi-stage systems with higher effectiveness and lower energy use.

VII. REFERENCES

[1] S. Dehghani, A. Date, and A. Akbarzadeh, “Performance analysis of a heat pump driven humidification-dehumidification desalination system,” *Desalination*, vol. 445, pp. 95–104, Nov. 2018, doi: 10.1016/j.desal.2018.07.033.

[2] H. Xu, Y. Zhao, and Y. J. Dai, “Experimental study on a solar assisted heat pump desalination unit with internal heat recovery based on humidification-dehumidification process,” *Desalination*, vol. 452, pp. 247–257, Feb. 2019, doi: 10.1016/J.DESAL.2018.11.019.

[3] H. Ge, Y. Cai, P. Kang, J. Liu, and X. Liu, “Experimental Study on Humidifier Performance in a Humidification-Dehumidification System,” in *Journal of Physics: Conference Series*, IOP Publishing Ltd, Feb. 2022. doi: 10.1088/1742-6596/2186/1/012027.

[4] Z. Rahimi-Ahar, M. S. Hatamipour, and L. R. Ahar, “Air humidification-dehumidification process for desalination: A review,” *Prog Energy Combust Sci*, vol. 80, p. 100850, Sep. 2020, doi: 10.1016/J.PECS.2020.100850.

[5] D. U. Lawal and N. A. A. Qasem, “Humidification-dehumidification desalination systems driven by thermal-based renewable and low-grade energy sources: A critical review,” *Renewable and Sustainable Energy Reviews*, vol. 125, p. 109817, Jun. 2020, doi: 10.1016/J.RSER.2020.109817.

[6] A. E. Kabeel and M. Abdelgaied, “Experimental evaluation of a two-stage indirect solar dryer with reheating coupled with HDH desalination system for remote areas,” *Desalination*, vol. 425, pp. 22–29, Jan. 2018, doi: 10.1016/J.DESAL.2017.10.016.

[7] S. Hussain Soomro, R. Santosh, C. U. Bak, C. H. Yoo, W. S. Kim, and Y. D. Kim, “Effect of humidifier characteristics on performance of a

small-scale humidification-dehumidification desalination system," *Appl Therm Eng*, vol. 210, p. 118400, Jun. 2022, doi: 10.1016/J.APPLTHERMALENG.2022.118400.

[8] Q. Zhu, W. Wu, Y. Ren, F. Wang, and Y. Han, "Study on the Heat and Mass Transfer Characteristics of Humidifiers in Humidification–Dehumidification Desalination Systems," *Energies (Basel)*, vol. 16, no. 24, Dec. 2023, doi: 10.3390/en16248006.

[9] Y. Zhang, H. Zhang, W. Zheng, S. You, and Y. Wang, "Numerical investigation of a humidification-dehumidification desalination system driven by heat pump," *Energy Convers Manag*, vol. 180, pp. 641–653, Jan. 2019, doi: 10.1016/j.enconman.2018.11.018.